Double image in far peripheral vision of pseudophakic eye as source of negative dysphotopsia

This is the author's Accepted Manuscript (AM). The final version is in the Journal of the Optical Society of America A, Vol. 31, Issue 12, pp. 2642-2649 (2014) https://doi.org/10.1364/JOSAA.31.002642

Michael J. Simpson

Simpson Optics LLC, Arlington, Texas, USA *Corresponding author: mjs1@outlook.com*

Received Month X, XXXX; revised Month X, XXXX; accepted Month X, XXXX;
posted Month X, XXXX (Doc. ID XXXXX); published Month X, XXXX

Some intraocular lens (IOL) patients report seeing "dark shadows" at visual angles that are larger than 60-70 degrees. Raytrace models of the pseudophakic eye show that light starts to miss the IOL at large visual angles because the implant diameter of about 6mm is much smaller than the natural crystalline lens diameter of 9.5 mm. This light forms a second displaced image on the peripheral retina. To evaluate the appearance of the image, raytrace software was used to image an illuminated window onto the highly curved retina, and a method was developed to project the image back to object space for evaluation on a flat surface. Only a single schematic eye was evaluated monochromatically, and the low resolution of the peripheral retina was not modeled, but the simulated images depict a shadowlike phenomenon at similar visual angles to reports of "negative dysphotopsia".

 OCIS codes: (330.4060) Vision modeling; (330.7326) Visual optics, modeling; (330.5370) Physiological optics

1. Introduction

"Dark shadows" are occasionally reported by intraocular lens (IOL) patients in extreme peripheral vision, particularly in the early postoperative period[1,2]. These have been described in the literature as dark crescent-shaped shadows in the temporal direction[3], and they are not typically reported in the nasal, inferior or superior directions. Various potential causes have been suggested, and there have been several case reports and evaluations of the topic[1-8], in addition to proposed modifications to IOLs[9-12]. These publications indicate that there are many potential mechanisms that may create a shadow, and that it is possible that not all reports of dark shadows have the same cause. Dark shadow phenomena are generally grouped together under the term "negative dysphotopsia", in contrast to the term "positive dysphotopsia" that is used to describe bright unwanted visual phenomena. There is a general consensus that the primary *positive* dysphotopsia phenomenon from IOLs[1] is due to light reflected from the edge of an IOL, which creates an arc-shaped image close to the fovea at night. There is no similar consensus on the primary cause of negative dysphotopsia[13-15].

There appears to have been relatively little research into vision for the "far" peripheral region of the eye. "Peripheral vision" is a phrase that is often used to describe vision just outside the main foveal region of the eye, where visual acuity is still relatively high. The dark shadows that are reported are typically at visual angles of over 60 or 70 degrees, however, which is sometimes called "far" peripheral vision[16]. Visual acuity is not normally tested for this region of the retina, and although visual fields are sometimes tested at very large angles, this is usually to identify pathology, rather than to evaluate visual capabilities. This is a region of the retina with very low resolution, but it is extremely sensitive to motion[16]. A slight hint of something moving in the far periphery can create a response so that the eye or head can rotate to evaluate the location with closer scrutiny.

Dark shadows are not reported by phakic patients who have a natural crystalline lens, and the pseudophakic patients who report the phenomenon are the only observers who can characterize it. The phenomenon is described as being a "shadow", but this paper demonstrates that the pseudophakic eye can have a "shadowlike" phenomenon due to imaging characteristics, rather than to an actual "shadow" where the light has been obstructed. The main cause of this has already been included in several publications that have used raytracing to evaluate possible shadow causes, but evaluations of the shadow as an imaging phenomenon have been limited. The raytracing shows that the point spread function (PSF) has two strong peaks[4,6,9-11], because a large crystalline lens is replaced by a much smaller synthetic intraocular lens (IOL). At very large visual angles some of the light misses the IOL completely, and it forms a second image. The overlap region between the two images has the appearance of a shadow, but there is no standard method for creating and displaying images for the far peripheral vision region of the eye. The location of the double-image "shadow" is largely at a fixed location relative

to the eye, which is in agreement with patient observations. As the eye continuously moves, the image structure will typically vary, but the impression will be given of a darker arc-shaped region at a specific angular location.

The paper by Holladay et al[4,15] provides an excellent review of various aspects of negative dysphotopsia, along with results from raytrace calculations for specific IOL designs that consider light paths through the edge of the IOL optic to be important. Unfortunately, the edge designs evaluated do not appear to include the physical characteristics of the edges of the AcrySof IOLs that are identified in the paper as creating negative dysphotopsia. Electron micrographs of actual AcrySof IOLs are depicted in several publications[17-20] where it can be seen that the edge profiles are both curved and highly diffuse. These are features that minimize the visibility of *positive* dysphotopsia by preventing strong reflections from the IOL edges, and they also defocus and scatter light passing through the lens edge. Raytracing these lens edges as simple cylinders would give spurious results, because the edges are both toroidal and highly diffusing. Light incident on the lens edges can be considered to be highly scattered, and can be ignored. In addition, there is a misleading conclusion in the same paper that light that misses the IOL cannot be a contributing factor to negative dysphotopsia. In figure 4 of the paper, however, a ray that just misses the IOL could be drawn from the lowest edge of the iris to a retinal point at about -100 degrees of retinal field angle (though this ray is not drawn in the figure). This is well within the range of the useful retina, yet a discussion in the paper states the opposite.

This paper builds on the earlier work by creating visual images that display a clear "shadow", using the two primary imaging components. The image is formed on a curved retina, and a method is developed to display the image on a flat surface for evaluation. The image is expressed in terms of input visual angle, and a square physical window is used as a representative object. This primarily models only a monochromatic image that is incident on the retina, and it does not model how the visual system processes the image. The eye can easily be rotated to place the object at different visual angles, and the appearances of the image for different horizontal angular rotations are compared.

2. Method

The main light paths that create a double image with an intraocular lens are depicted in Figure 1 using a schematic eye that is similar to one used by Holladay et al [4], with a 4 mm diameter pupil, and a separation of 1 mm between the iris and the IOL. The entire beam of light that enters the eye is focused by the cornea, but at large visual angles only part of the light beam is focused by the IOL. Some of the light misses the IOL, and because it does not experience the additional focusing power of the IOL, it creates a second image at a more peripheral location on the retina. This image is typically larger than the primary image, and with a different level of defocus.

Dark shadows are reported for the temporal visual field, rather than any other direction. This is probably because the nose, eyebrow, and cheek generally prevent light entering the eye at large visual angles from other directions when the eye is looking forward. This is indirect confirmation that the dark shadow phenomenon is caused by light at large visual angles.

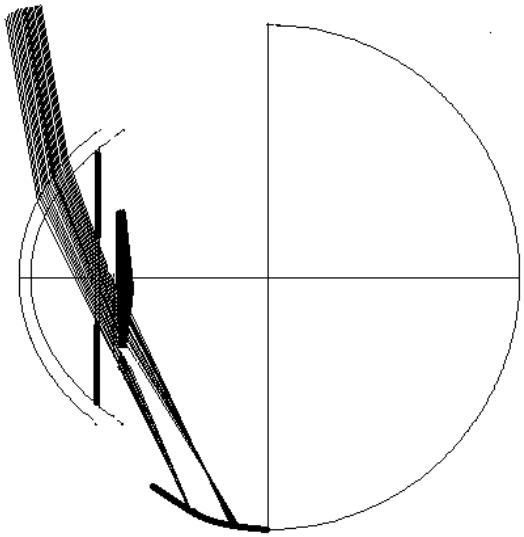

Fig. 1. Light rays entering a pseudophakic eye at a large visual angle. After passing through a 4mm diameter iris, part of the light is focused by the IOL and part of it misses the IOL, which creates a displaced second image.

Dark shadows are also primarily a daytime phenomenon rather than a night-time phenomenon, with normal daytime pupil diameters. This indicates that the cause is probably due to light from extended objects rather than point sources. At night there are many bright point sources, such as headlights and streetlights, and other brightly lit signs in the typical urban environment, and these do not appear to lead to reports of dark shadows ("negative dysphotopsia"), though bright light sources at night are a known cause of "positive dysphotopsia". During the day, however, bright point sources of light are rare, and they are not typically mentioned when dark shadows are observed.

Even though Figure 1 illustrates two focused image locations with a gap between them, it does not directly depict an extended "shadow" because only a point source is imaged. Similar figures are also included in other references that discuss dark shadows, where light from a single point source is divided into two image points. The eye is actually an unusual optical system for this imaging region, and for large visual angles the image is formed on the retina in the front hemisphere of the eye. The rays are traveling very obliquely through the pupil, and the image "point spread function" (PSF) from a single object point has two peaks, and the PSF characteristics vary as the visual angle changes. The level of vignetting for the two images gradually changes with the angle, while both the energy transmitted through the oblique pupil, and the level of defocus, are also changing. This is very different from conventional imaging, where optical systems are typically assumed to be "isoplanatic" over a large region of the image, with the PSF identical at every point. The focused energy gradually moves from one image to the other as the visual angle increases for this far peripheral vision region of the pseudophakic eye.

One purpose of this paper is to generate images that demonstrate a shadowlike phenomenon for peripheral vision. There is no standard method for displaying images for this region

of the eye, and the most common evaluation of the peripheral retina is the visual field test. This evaluates the threshold ability to sense light at different visual angles, and the results are plotted on a circular plot of visual angle, but no image is generated. The concept that is explored in this paper to illustrate the shadow is to consider a patient sitting in a room with normal daytime illumination. The room has a window, and the patient can swivel horizontally to either look towards the window or to look away from it, and can rotate to any angle in-between. It turns out that a distinct shadow-like image is created by the image from the strong light-to-dark transition at the vertical window edge. This type of vertical visual object is common in the general environment, such as the walls of buildings, trees, doorways, grocery store shelving units, etc., but an illuminated window provides a convenient object for theoretical evaluation.

Visual acuity is extremely poor for far peripheral vision, and even if an image is present on the retina it is not necessarily observed very accurately. The retina has relatively few rods in the far periphery, and the signals from the retinal sensors are combined by the brain to create a representative image of the scene, with an important aspect being the ability to detect motion rather than to resolve the image [16]. The eye usually concentrates on the images that are formed more centrally. The eye can always be rotated to view the object directly, but it can glance back and forth at will comparing the actual object to the more general impression that the user has of the object that is in their peripheral vision. These would be expected to be in agreement with each other, though the actual details of how the brain interprets the image, or how well the object is resolved peripherally, are not modeled in this paper.

To simulate the image that is incident on the retina so that it can be evaluated on the printed page, or on a display screen, the image is scaled here in terms of visual angle in object space. The image is initially formed on the highly curved retinal surface, and a relationship was developed using a model of a schematic phakic eye that contains a human crystalline lens (Figure 2) to relate retinal locations to visual angles. This addresses the scaling problem with the pseudophakic eye where a single object point is

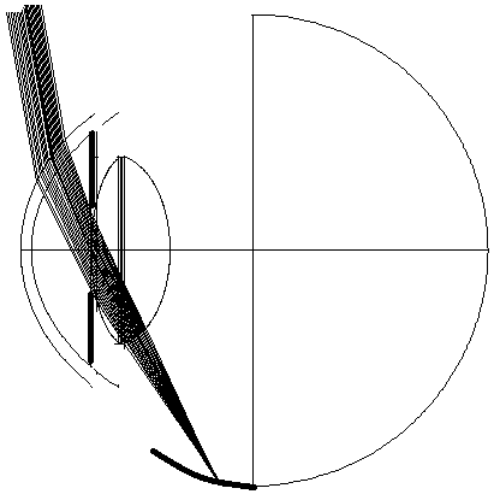

imaged simultaneously at two separate locations on the retina.

Fig. 2. Light rays entering a phakic eye at a large visual angle. The crystalline lens is modeled using a gradient refractive index material and conic outer surfaces

The Zemax raytrace software (Radiant Zemax, Redmond, WA) was used to evaluate the schematic eyes. The imaging capabilities of the software were used, where an object that covers a square field of view can be specified in angular units. The software does not directly create an appropriate image that can be viewed, however, and a Zemax macro was written to determine the ray intersections with a spherical retina. The intersection points were written to a file, and then imported into Matlab (Mathworks, Natick MA) for analysis and display. The use of a perfectly spherical retina is very convenient for simplifying the analysis, and it is a reasonable approximation to the actual human eye.

The schematic model eye and IOL that were used were very similar to the one described in Holladay et al [4]. This has a corneal power of 43.5 D, an anterior cornea conic constant Q value of -0.26, ACD from anterior cornea to anterior IOL of 4.6 mm, pupil diameter of 4mm, and an acrylic IOL with material index 1.550, power of 20 D, anterior surface power 7 D, center thickness 0.63 mm, and diameter of 6mm. The IOL edge is assumed to be rounded and roughened, so that it would defocus and scatter light rather than focus it, and it is not included in the evaluation. The distance from the iris to the IOL was 1mm, and the iris was thin. The retinal surface was assumed to be a 12 mm diameter sphere, with the center located at 11.84 mm from the corneal apex. The Zemax model eye was rotated by 90 degrees in order to record retinal image locations out to large visual angles. This addressed a characteristic of Zemax, but visual angles were expressed conventionally.

The sides of the square object that was used for evaluation covered a visual angle of 10 degrees. This is similar to viewing a 1 meter square window at 6 meters, or a 0.5 meter square window at 3 meters. The primary focused image was calculated for light that passed through the anterior IOL surface. A secondary calculation was made at large visual angles using rays that missed the anterior and posterior IOL surfaces, and this created the second displaced image. This provided the ability to view the image components either separately or together, with the same relative scaling. Any vignetted rays that were obstructed before reaching the retina were tracked and used to scale the ray intensities of the focused images. The imaging calculation in the Zemax raytrace software always attempts to trace the same number of rays within the entrance pupil for all the visual angles, even though the apparent aperture diameter decreases as the visual angle increases (the effective pupil area decreases by approximately the cosine of the incident angle[21]). No compensation was made for this, since this is also a characteristic of the phakic eye that is used for comparison, and it forms part of the retinal response characteristics that are not being modeled.

The reference for the visual angle calculations was determined for a phakic eye, where the IOL was replaced by a crystalline lens that was based on the gradient index model described by Liou and Brennan[22]. This was not originally intended to be used at very large visual angles, but adjusting the anterior surface conic to 5.5 and the posterior surface conic to 1.8 created a crystalline lens that had the cross sectional appearance of a natural crystalline lens (Figure 2). The axial location was adjusted to make the eye emmetropic. A comparison of the eye with the crystalline lens, and the same eye with the IOL, showed that image locations were

generally similar up to 70 degrees of visual angle (where the IOL image bifurcates, and there is no unique relationship between object and image locations). This simplified model continues the scaling out to 90 degrees, which provides the ability to compare the peripheral images of the phakic and the pseudophakic eye. Other more sophisticated models for the crystalline lens have been published[23,24], but it is not clear that they have been verified for their imaging properties at very large visual angles, and the simpler model was used instead.

An initial evaluation explored how the ray intersections with the retina would need to be adjusted in order for a square object to appear square on the final displayed image using the phakic eye model. This led to a relatively straightforward calculation for adjusting the ray image locations, which is similar to compensating for "distortion" effects for conventional imaging. Other authors have defined a "retinal field angle", which gives the angular distance, subtended at the center of the retinal sphere, of a ray intersection relative to the fovea [4,6]. A similar approach was taken as the starting point here, where the longitude and latitude of the ray intersections on a spherical retina were converted to visual angles outside the eye, using the terminology that is commonly applied to the distances around the earth, with the fovea at 0 degrees for both directions. The main direction of interest is the horizontal direction that goes out to a large visual angle, and conversion equations were calculated using chief rays (the rays that go through the center of the pupil) for a range of horizontal visual angles, for both 0 degrees and -5 degrees vertically. Only a small square object is being imaged, and the method used was to scale the horizontal axis directly, and then to determine a vertical scaling function which made a 5 degree vertical field point have the correct value. The same vertical scaling was then used proportionally for all other vertical field points.

The final images were created by adding rays to a standard rectangular image that was 1000 pixels wide and 200 pixels tall, covering visual angles from -10° to +90° horizontally, and from -10° to +10° vertically. The ray contributions were simply added for each pixel. There are occasional artifacts in the images due to the choices of the number of rays, and the sampling method, but these do not detract from the shadowlike characteristics that are being evaluated.

3. Results

The relationship between the retinal intersection in image space, and the horizontal input visual angle of the chief ray, is plotted in Figure 3 for the phakic eye. Visual angles are positive, and the angles at the retina are negative because the image is inverted. This relationship can be used to convert the retinal image location back to an object space visual angle. This is a remarkably linear relationship, considering the steep curvature of the retinal surface, and the fact that the imaging region covers more than 90 degrees. The input visual angle is about ¾ of the retinal angle subtended at the sphere center. The relationship does not monitor whether the image is in focus or not, but it characterizes where the central ray intersects the retina.

The vertical dimension of the square object was rescaled using the relationship depicted in Figure 4, using a different method. This plot gives the latitude angle at the retina for a chief ray from an object point at -5 degrees, which corresponds to the half height

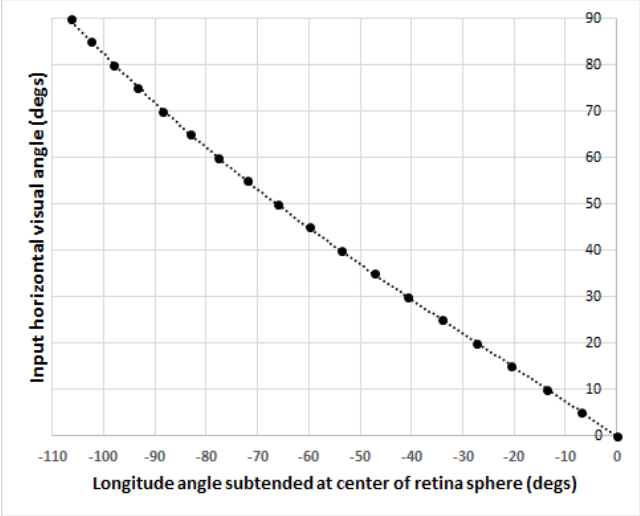

of the window being imaged. Vertical heights were scaled in proportion to this plot.

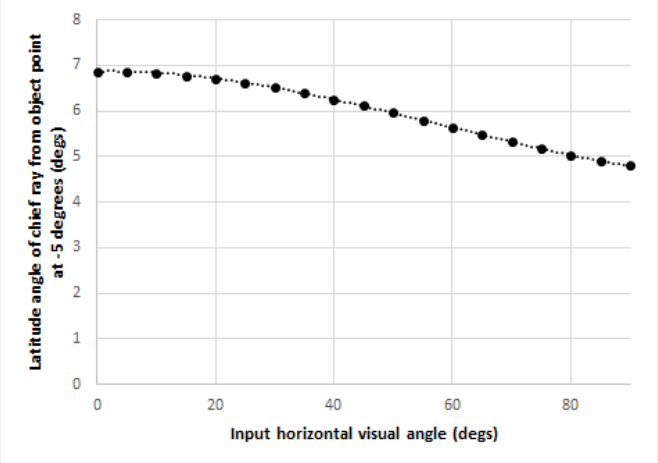

Fig. 3. Relationship between the input chief ray horizontal visual angle and the longitudinal image angle subtended at retinal sphere center for a phakic eye.

Fig. 4. Latitude angle scaling curve.

Cubic equations were used to rescale the images from the curved retina to a flat representation of object visual field angle using the data from Figure 3 and Figure 4. The equations are:

$$\text{Horizontal visual angle} = -0.00002197*x^3 - 0.0016021*x^2 - 0.764605*x \quad (1)$$

$$\text{Vertical visual angle} = y * 5/(0.0000033197*x^3 - 0.000584587*x^2 + 0.00255444*x + 6.8721) \quad (2)$$

where x is the longitudinal angular distance from the fovea in degrees subtended at the center of the spherical retina, and y is the latitude angle. The denominator of equation 2 is the curve plotted in Figure 4, which gives the image height in degrees for an input visual angle of -5 degrees vertically as a function of visual angle. This method assumes that the scaling is proportional for

other values of y in the range of interest. The image height drops by about ¼ from the fovea to the 90 degree field angle.

Images for the phakic eye of the 10 degree square object centered at horizontal field angles of 0, 20, 40, 60, and 80 degrees are superimposed in Figure 5(a). The total image field illustrated covers visual angles from -10° to +90° horizontally, and from -10° to +10° vertically. The individual images are all approximately square, which verifies that the calculations convert the retinal image locations back to object-space visual angles. The image at the 80 degree visual angle has some aberration in the vertical direction, and a modest reduction in width, and there are also occasional artifacts due to sampling effects in many of the images.

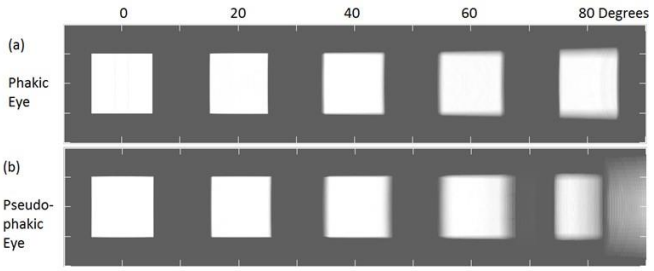

Figure 5. Images on the retina rescaled back to object space and superimposed, with each large rectangular image representing visual angles from -10 to +90 degrees horizontally and from -10 to +10 degrees vertically. A square object that covers 10 degrees of visual angle was imaged centered on visual angles of 0, 20, 40, 60, and 80 degrees. (a) Phakic eye. (b) Pseudophakic eye.

For display, the intensity of each sub-image was first normalized to a value slightly larger than the peak sub-image intensity, an intensity offset was added to simulate very dim room illumination, and a gamma value of 0.3 was used to compensate for typical printing and display properties. This image can be thought of as representing the eye viewing a window, with images on the retina snapped at different rotation angles. The window appears approximately square on the retina using this representation, but the retina/brain combination has a resolution that declines significantly with increasing rotation angle, and the object will not typically be perceived as clearly as this, particularly in the region of far peripheral vision. This evaluation displays the image that is available on the retina, however, and it is represented in terms of visual angle in object space in a simple rectangular image format.

When the crystalline lens is replaced by the IOL, the results for the same visual angles are given in Figure 5(b). The first four angles have broadly similar image characteristics, which indicates that imaging with an IOL is broadly similar to imaging with the crystalline lens, though there is additional aberration in the horizontal direction for this particular IOL at 60 degrees, in addition to a very faint hint of an extra image to the right. At the larger 80 degree angle however, the right hand side of the main focused image is missing, and there is a prominent additional image component on the right from the light that was not focused by the IOL.

The far peripheral vision region is evaluated in more detail for the pseudophakic eye in figures 6 and 7 for different values of visual angle. Figure 6 gives images for a series of large visual angles that are 5 degrees apart, with the object centered on visual angles from 60 to 85 degrees. These images all include the light that misses the IOL (but not light that hits the lens edge, which is presumed to be scattered, and to only contribute to a very faint background light level). In each part of the figure the rectangular field illustrated covers the same region of visual angle as in Fig. 5 (-10° to +90° horizontally; -10° to +10° vertically). The second image is displaced from the primary image, and it is larger because it has not experienced the additional power of the IOL.

Figure 6. Images on the retina of the pseudophakic eye rescaled back to

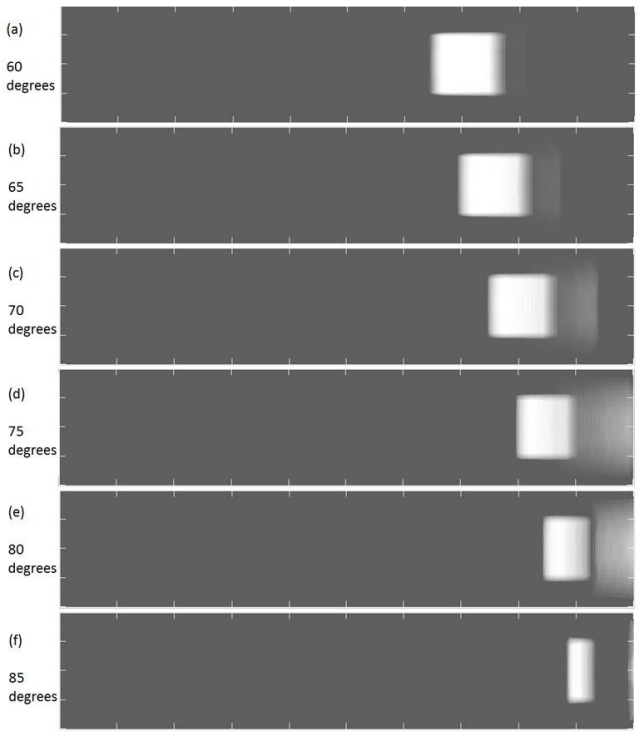

object space, with each large rectangular image representing visual angles from -10 to +90 degrees horizontally and from -10 to +10 degrees vertically. The 10 degree square object was centered on the following horizontal visual angles in degrees: (a) 60, (b) 65, (c) 70, (d) 75, (e) 80, and (f) 85. The main image is light focused by the IOL, and the image to the right is the light that misses the IOL.

Even for the smaller visual angles, such as 65, 70 or 75 degrees, the right hand side of the primary image might be thought of as having a shadow, because of the intensity change from the main image to the secondary peripheral image. The image at 80 degrees has a very definite dark region between the two image components. None of these characteristics are actually shadows, but this is a low resolution region of the retina, and they would visually appear as "dark shadows".

Figure 7 contains additional images that cover the most shadowlike angular region from 74 to 84 degrees. The angular changes between the images have been reduced to 2 degrees. The image at 80 degrees is included again, and it can be seen that the dark region increases in width between the 82 and 84 degree images.

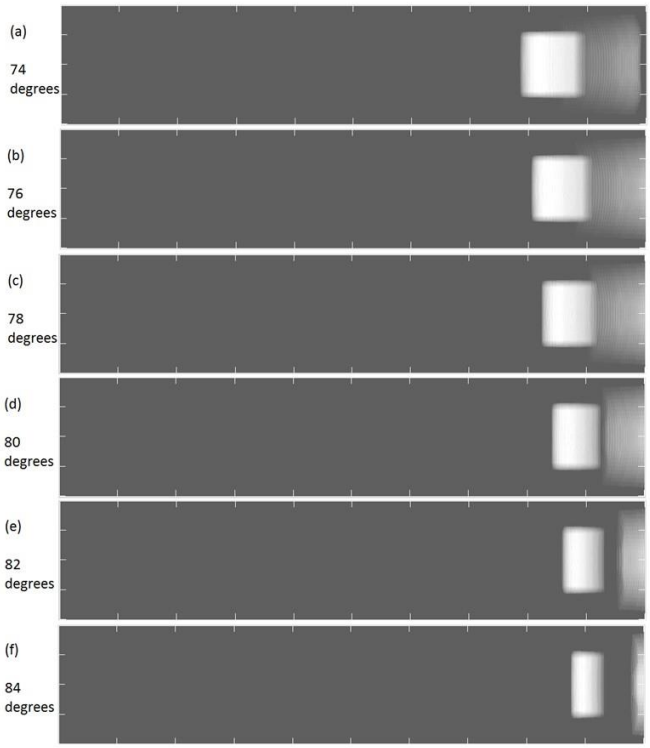

Figure 7. Images for the pseudophakic eye similar to Figure 6, with the square object centered on alternative horizontal visual angles in degrees of: (a) 74, (b) 76, (c) 78, (d) 80, (e) 82, and (f) 84.

4. Discussion

The images indicate that a shadowlike phenomenon on the peripheral retina is an expected consequence of the use of an IOL, even though this is rarely perceived. The "shadow" occurs because some of the light that enters the eye at large angles misses the IOL, and a shifted secondary image is created. The overlap between the two images, or an actual gap between them for smaller objects, can give the appearance of a shadow. This is primarily an imaging phenomenon, rather than an actual shadow that is cast by an opaque object somewhere in the optical path. The shadow appearance is probably exaggerated by an object that has a strong vertical change in luminance, such as a window or door, and less obvious for a point light source, or for a continuous illuminated field.

A relatively large separation between the iris and the IOL has been modeled here, which makes the shadow very prominent for a smaller object. However, even though the PSF and the images of the particular object evaluated here change with visual angle, the main "shadow " region is primarily fixed relative to the eye. The eye is in continual motion, and as the structure of objects in the far peripheral region move across the retina, the average impression will be of a peripheral shadow.

Very few IOL patients report this phenomenon as a persistent observation, and often it is only experienced in the initial postoperative period. The eye has very poor acuity in far peripheral vision, and limited attention is given to this region of the visual field. There were no clinical reports at all of dark shadows with older rigid IOLs, which indicates that improvements to overall surgical methods, in addition to IOL designs, have made this phenomenon visible. Older surgical methods created significantly more capsular haze, which would tend to obstruct the optical path to the periphery, and also scatter light into the peripheral image region that would reduce visibility of the shadow. Increased corneal aberrations due to the larger incisions for PMMA IOLs may also have had an effect. The introduction of phacoemulsification, a strong emphasis on cleaning the capsule, and the introduction of foldable lenses with a sharp posterior optic edge, have all increased the clarity of the capsule. Foveal vision has improved because of these changes, and this has also led to improved image quality in the periphery. Some patients report seeing dark shadows in the immediate postoperative period, and then later they are not observed. This is consistent with both adjusting to the phenomenon, and with increased scattering within the eye over time making it less obvious.

Most of the methods that have been used clinically to reduce the visibility of dark shadows are consistent with the double-image concept [3,-5,7-8,14-15]. Generally, anything that alters the light path for the far peripheral vision region will alter the appearance of the peripheral image. This includes such things as introducing a second IOL into the anterior chamber, changing the IOL for an alternative lens style, using an IOL in the sulcus rather than the capsular bag, rotating the haptics so that the haptic-optic junction is in the temporal region, adjusting lens centration, and making changes to the capsule. These reduce shadow visibility by reducing the gap between the iris and the IOL, by adding additional lens material between the iris and the IOL, and by increasing the scattering material in the region outside the IOL.

A non-surgical method to reduce the visibility of negative dysphotopsia may be to use spectacles as a distraction, though this is less attractive for a patient who desires to have a reduced dependence on spectacles. Adding spectacles provides an additional element in the visual field that might reduce the sensitivity to the dark shadow. The frames of spectacles themselves are always visible to spectacle users, who have no trouble tolerating their continuous presence. The frame illumination changes as the head moves, and the visual angle to the eye changes when the eye and the head are rotated with respect to each other. The peripheral dark shadow phenomenon may be a more bothersome artifact than a spectacle frame if it is observed because it appears to change the object itself, with no apparent physical cause.

One prominent characteristic of clinical reports of dark shadows that is not illustrated by the simulated images is that the shadows are often described as being curved and arc-like rather than straight. This is probably because of the use here of a single square object of limited extent in order to demonstrate a distinct shadow, and the way that the intensity is adjusted using the Zemax image calculation. The overall shadow would be expected to be curved because the double image varies with radial angle. In a more general everyday environment, the continuous change in object scenery as the eye rotates would lead to a distinct impression of a "shadow" at a relatively fixed angular location in-between the two images. The changes in the shadow structure with eye motion would make the shadow region more visible.

There are also other factors in this visual region that may affect the perception of curvature. For example, the very extreme limit of the visual field is itself curved, and a peripheral vertical shadow may appear to be curved if it has limited height. There are also difficulties with describing the characteristics of the "shadow" itself, which is poorly resolved in peripheral vision. Patient

sketches are often drawn on top of a sketch of the eye (rather than depicting the scene outside the eye), or on a circle. The appearance of straightness for a vertical object in the far peripheral visual field may actually never have been explored, even for phakic subjects. For example, if the eye is presented randomly with straight or curved objects in the peripheral visual field, are they perceived as straight or curved, and how sensitive is the judgment of this? In addition, a premise for the modeling method used here is that a square image should always appear square, but this may actually be incorrect.

The paper by To et al [16] includes measured data for peripheral contrast sensitivity which indicates for phakic subjects that at 80 degrees of visual angle, sensitivity to moving gratings is highest for spatial frequencies below about 0.5 cycles per degree. This spatial frequency range is similar to the distinct dark bar that is visible in the Figures for about the same visual angle. The eye moves continuously, and it is possible for the eye to keep returning to the angle and the rotation speed that make the phenomenon most visible. Sensitivity is much lower to stationary targets, and the phenomenon should be much less visible when the eye is stationary.

Various simplifying assumptions have been made in this initial evaluation, and only a single schematic eye has been evaluated. Variations in eye parameters, such as corneal power, anterior chamber depth, iris location, iris thickness, pupil diameter, IOL centration, IOL design, asymmetries in the optical system, refractive error for peripheral vision, etc., may make a shadow more or less prominent. Also, if the gap between the iris and the IOL is eliminated completely, that would tend to reduce the total visual field, which may be an additional source of some dark shadow reports.

Various publications discuss additional modeling methods for the eye [25-29], but they do not typically include a method to represent the appearance of the image. The simplified scaling method developed here was created to provide a representation of the overall image that is available for the retina to evaluate, while not extending the model to simulate what the eye might actually perceive. The method essentially includes an implicit control, however, because the eye can always rotate to look at the object directly, which allows the peripheral image to be compared to the direct image.

Other publications that use raytracing to model negative dysphotopsia do not appear to generate retinal images for typical objects. For example, a point source was used by Hong et al [6,13], and a Ganzfeld source and individual rays were used by Holladay et al[4,15]. It is not clear how Hong et al[6] modeled the IOL edge in their calculations, though surface/edge reflections are included in the image plots, which include extremely faint surface reflections. The paper by Holladay et al[4] does not evaluate an IOL that has the curved and diffuse edge profile modeled here, as discussed in the introduction. Also, although figure 3 in the same paper might be interpreted to represent shadows on the retina for Ganzfeld illumination, this may be a pictorial representation of the locations of ringlike shadows from table 1 and elsewhere, rather than a simulated image. The main image intensity does not appear to vary in the plot, even though the intensity transmitted through the oblique pupil should decrease significantly at larger visual angles. The concept of a double image is not directly evaluated in these publications, nor is the gradual change in the imaging properties with visual angle. Any values for "retinal field angles" in these publications can be approximately converted to visual field angles using a multiplier of 0.75 (from equation 1 above).

The shadow effect due to the double image is generally much stronger than any of the other potential sources of shadows. At the angle where the illumination bisects the edge of the IOL, about half of the focused light is used to form each of the two images, and most of the imaged light intensity is contributing to the shadow. The effects of reflected light would be much fainter, and any structure that actually casts a shadow on the retina would also only affect a very small portion of the available illumination.

The use of IOLs started empirically with cataractous crystalline lenses being replaced by IOLs because vision was no longer possible. IOLs have since seen widespread use, with no particular clinical problem being found with either peripheral vision, or "far" peripheral vision, in everyday life. If a similar activity were to be started today, calculations similar to those in this paper would probably be made. The calculations indicate that the image on the retina in the far peripheral vision region is different to the image when using a natural crystalline lens, with a distinct double-image. Without clinical data, it would not be clear how significant this would be to a person using an IOL.

The clinical reports of "dark shadows" actually appeared without any prior calculations, and although the demonstration in this paper that the peripheral double image can have the appearance of a shadow, this does not prove definitively that the double image is actually the source of clinical dark shadow reports. The evaluation provides a basis for additional work, however. The visual angle of the shadow could be measured clinically, for example, and this could be compared to a simulated value for each specific eye. The difference in visibility of primary targets such as illuminated point sources, line targets, edge targets, bar targets, and a completely white field (Ganzfeld) should also provide useful information.

Meanwhile, even when the defocused light misses the IOL in a pseudophakic eye, any movement in the periphery will still attract attention, which is perhaps the main purpose of far peripheral vision. Patients who see dark shadows are already being assured that the symptoms will not progress, and that they will typically decrease over time. An improved theoretical understanding of far peripheral vision should provide additional support for this assurance.

References

1. J. A. Davison, "Positive and negative dysphotopsia in patients with acrylic intraocular lenses," J. Cataract Refract. Surg. **26**, 1346-1355 (2000).
2. W.B. Trattler, J. C. Whitsett, P. A. Simone, "Negative dysphotopsia after intraocular lens implantation irrespective of design and material," J. Cataract Refract. Surg. 31, 841-845 (2005).
3. R. H. Osher, "Negative dysphotopsia: long-term study and possible explanation for transient symptoms," J Cataract Refract Surg. **34**, 1699-1707 (2008).
4. J. T. Holladay, H. Zhao, C. R. Reisin, "Negative dysphotopsia: the enigmatic penumbra," J. Cataract Refract. Surg. **38**, 1251-1265 (2012).
5. S. Masket, N. R. Fram, "Pseudophakic negative dysphotopsia: Surgical management and new theory of etiology, " J. Cataract Refract. Surg. **37**, 1199-1207 (2011).
6. X. Hong, Y. Liu, M. Karakelle, S. Masket, N. R. Fram, "Ray-tracing optical modeling of negative dysphotopsia," J. Biomed. Opt. **16**, 125001-1-7 (2011).

7. D. L. Cooke, S. Kasko, L. O. Platt, "Resolution of negative dysphotopsia after laser anterior capsulotomy," J. Cataract Refract. Surg. **39**, 1107-1109 (2013).
8. E. R. Burke, L. Benjamin, "Sulcus-fixated intraocular lens implantation for the management of negative dysphotopsia," J. Cataract Refract. Surg. In Press. (2014)
9. M. J. Simpson, D. Stanley, X. Zhang, S. K. Ellis, US Patent Application 2008/0269886 A1, "IOL peripheral surface designs to reduce negative dysphotopsia".
10. M. J. Simpson, US Patent Application2008/0269889 A1. "Haptic junction designs to reduce negative dysphotopsia".
11. M. J. Simpson, X. Zhang, US Patent Application 2008/0269890 A1, "IOL with peripheral region designed to reduce negative dysphotopsia".
12. S. Maskett, US Patent 8,652,206 B2. "Anti-dysphotopic IOL and method". (2014).
13. X. Hong, Y. Liu, M. Karakelle, S. Masket, N. R. Fram, "Negative dysphotopsia: differences in the studies of an enigmatic optic phenomenon," J. Cataract Refract. Surg.," **39**, 484-485 (2013).
14. S. Masket, N. R. Fram, "Etiology of negative dysphotopsia," J. Cataract Refract. Surg. **39**. 485-486 (2013).
15. J. T. Holladay, "Negative dysphotopsia: differences in the studies of an enigmatic optic phenomenon," Reply. J. Cataract Refract. Surg. **39**, 486.e1-e4 (2013).
16. M. P. S. To, B. C. Regan, D. Wood, J. D. Mollon, "Vision out of the corner of the eye," Vision Res. **51**, 203-214 (2011)
17. L Werner, M. Muller, M. Tetz, "Evaluating and defining the sharpness of intraocular lenses. Microedge structure of commercially available square-edged hydrophobic lenses," J. Cataract Refract. Surg. **34**, 310-317 (2008).
18. T. Brockmann, C. Brockmann, S Nietzsche, E. Bertelmann, J. Strobel, J. Dawczynski. "Scanning electron microscopic characteristics of commercially available 1- and 3-piece intraocular lenses," J Cataract Refract Surg. **39**:1893–1899 (2013).
19. M. Escobar-Gomez. D.J. Apple, L. G. Vargas, L Werner, S. N. Arthur, S. K. Pandey, A.M. Izak, J. M.Schmidbauer. "Scanning electron microscopic and histologic evaluation of the AcrySof SA30AL acrylic intraocular lens," J Cataract Refract Surg. **29**:164–169 (2003)
20. M. A. Nanavaty, D. J. Spalton, J. Boyce, A. Brain, J. Marshall. "Edge profile of commercially available square-edged intraocular lenses". J Cataract Refract Surg.**34**:677–686 2008.
21. D. A. Atchison, G. Smith, *Optics of the human eye* (Butterworth-Heinemann, Edinburgh, 2000).
22. H. L. Liou, N. A. Brennan, "Anatomically accurate, finite model eye for optical modeling," J. Opt. Soc. Am. A **14**, 1684-1695 (1997).
23. R. Navarro, F. Palos, L. González, "Adaptive model of the gradient index of the human lens. I. Formulation and model of aging ex vivo lenses," J. Opt. Soc. Am. A **24**, 2175-2185 (2007).
24. A. V. Goncharov, C. Dainty, "Wide-field schematic eye models with gradient-index lens," J. Opt. Soc. Am. A **24**, 2157-2174 (2007).
25. R. Navarro, "The Optical Design of the Human Eye: a Critical Review," J. Optom. **2**, 3-18 (2009).
26. P. K. Verkicharla, A. Mathur, E. A. Mallen, J. M. Pope, D. Atchison, "Eye shape and retinal shape, and their relation to peripheral refraction," Ophthalmic Physiol. Opt. **32**, 184-199 (2012).
27. D. A. Atchison, N. Pritchard, K. L. Schmid, D. H. Scott, C. E. Jones, J. M. Pope, "Shape of the retinal surface in emmetropia and myopia," Invest. Ophthalmol. Vis. Sci. **46**, 2698-2707 (2005).
28. A. De Castro, S. Ortiz, E. Gambra, D. Siedlecki, S. Marcos, "Three-dimensional reconstruction of the crystalline lens gradient index distribution from OCT imaging," Opt. Express **18**, 21905-21907 (2010).
29. M. Bahrami, A. V. Goncharov, B. K. Pierscionek, "Adjustable internal structure for reconstructing gradient index profile of crystalline lens," Opt. Lett. **39**, 1310-1313 (2014).